Comparative Analysis of Sentinel-3 and Terra MODIS Satellite Images for Air Temperature Observation in Denpasar Area

ABSTRACT

This study evaluates the air temperature products of Sentinel-3 and Terra MODIS satellite images, with the aim of determining the comparison results of Sentinel-3 and Terra MODIS satellite images for air temperature observations, and also to determine the minimum and maximum temperatures of the Denpasar area obtained using satellite images. Correlation relationship analysis and Root Mean Square Error (RMSE) were used to investigate the correlation and the degree of accuracy between the air temperature of satellite imagery and the air temperature of field observations. The results showed that Terra MODIS satellite imagery has better accuracy to BMKG air temperature compared to Sentinel-3 satellite imagery. Terra MODIS imagery has a correlation coefficient value of 0.95 and an RMSE value of 0.51, while Sentinel-3 satellite imagery has a correlation coefficient value of 0.78 and an RMSE value of 0.93, so it can be noted that Terra MODIS satellite images are better used in air temperature observations than Sentinel-3 satellite images. The results also showed that the minimum temperature detected by Sentinel-3 satellite images from 32 observations was 9.51°C on September 23, 2021 and the maximum temperature was 41.50°C on April 14, 2021. Meanwhile, in Terra MODIS satellite images from 32 observations, the minimum temperature was 20.57°C on September 23, 2021 and the maximum temperature was 37.08 on April 16, 2021.

***Keywords**: Sentinel-3, Terra MODIS, air temperature, RMSE, correlation analysis*

1. INTRODUCTION

An increase in air temperature has a significant relationship with natural conditions, development activities and human life patterns (comfort index) [1]. The limited number of meteorological and climatological stations in observing air temperature in the field causes less even air temperature information provided, therefore remote sensing technology is an alternative solution that can be used to observe air temperature evenly for all regions [2]. Remote sensing satellite technology products that can be used in the process of observing air temperature are satellite images equipped with electromagnetic wave spectrum (band) red, near infrared, and thermal infrared [3]. Some satellite images with high temporal resolution and equipped with thermal infrared bands are Sentinel-3 satellite images and Terra Moderate Resolution Imaging Spectroradiometer (MODIS) satellites. In observing air temperature using remote sensing technology, the first element that can be identified is surface temperature, therefore the surface

temperature obtained by remote sensing systems needs to be converted back into air temperature based on satellite imagery [4]. The results of air temperature observations on each satellite have different levels of accuracy, sothe study of the comparison of Sentinel-3 and Terra MODIS satellite images for air temperature observations needs to be studied.

1.2. Sentinel-3 Satellite Imagery

The Sentinel-3 satellite has 4 instruments, namely Sea and Land Surface Temperature Radiometer (SLSTR), Ocean and Land Colour Instrument (OLCI), Sar Radar Altimeter (SRAL) and Microwave Radiometer (MWR) [5]. Sentinel-3 SLSTR satellite imagery, has a low spatial resolution of 500 m to 1 km per 1 pixel, but has several advantages, namely the instruments provided in Sentinel-3 SLSTR, specifically designed for observation of the earth's surface temperature so that Land Surface Temperature (LST) data is available morning and night at the same time. Sentinel-3 SLSTR also has the ability to measure LST with an accuracy level of < 1 K, besides that Sentinel-3 has a high temporal resolution with a revisit time of less than one day at the equator [6]. The Sentinel-3 SLSTR has a medium spectral resolution with 11 bands.

1.3. Terra MODIS Satellite Imagery

Terra MODIS satellite imagery is a National Aeronautics and Space (NASA) mission. Terra satellite has 5 sensors, the five sensors are Advanced Spaceborne Thermal Emission and Reflection Radiometer (ASTER), Clouds and the Earth's Radiant Energy System (CERES), Multi-angle Imaging Spectro Radiometer (MISR), Moderate-resolution Imaging Spectroradiometer (MODIS) and Measurements of Pollution in the Troposphere (MOPIT) [7]. TheTerra elite passes from north to south of the equator [8]. The Terra satellite passed at an altitude of 705 km and crossed the equator in the morning local time, at around 10:30 AM. Terra MODIS satellite has a fairly high temporal resolution product, which ranges from 1 day to 2

days, with a low spatial resolution ranging from 250 m to 1000 m, and has a high spectral resolution with a number of bands that are 36.

1.4. Imagery-Based Air Temperature Analysis

Please note that in remote sensing with thermal band satellite images, the first element that can be identified is surface temperature, so it is necessary to do several stages first to obtain air temperature data. According to Yang et al (2019) [9], Trebs et al (2021) [10] and Obisesan and Jegede (2022) [11] the equation to determine air temperatures (T_a) is as follows:

$$T_a = T_s - \left(\frac{Hr_{aH}}{\rho_{air} C_p}\right) \quad (1)$$

Information:

T_a : Air Temperature (K)

T_s : Surface Temperature (K)

H : Air Heating Flux (Wm^{-2})

ρ_{air} : Air Density (1,27 kgm^{-3})

C_p : Specific heat of air at constant pressure (1004 $Jkg^{-1}K^{-1}$)

r_{aH} : Aerodynamic resistance (sm^{-1})($31,9u^{-0.96}$)

Aerodynamic resistance is a function of wind speed. The greater the wind speed, the smaller the aerodynamic resistance that inhibits heat flux [12]. In the aerodynamic resistance equation there is (u) where (u) is the wind speed. Normal wind speed at a height of 1 m to 2 m is about 2 ms^{-1}. Wind speed values are differentiated in three land covers: water (2.01 ms^{-1}), non-vegetation (1.79 ms^{-1}) and vegetation (1.41 ms^{-1}). To find the value of H (air heating flux), Equation (2.1), Bowen Ratio value, net radiation and soil heat transfer can be seen in Table 1 and Table 2 [13]:

$$H = \frac{\beta (R_n - G)}{1 + \beta} \quad (2)$$

Information:

H : Air Heating Flux (Wm^{-2})

R_n : Net radiation (Wm^{-2})

β : Bowen ratio

G : Soil heat transfer (Wm^{-2})

Table 1 Bowen Ratio values for each land cover class

No.	Land Closure	Bowen Ratio
1.	Settlement	4,0
2.	Plantation	0,5
3.	Water	0,11
4.	Paddy	0,25
5.	Tropical Forest	0,33

Table 2 Rn and G values of heat transfer for each land cover

No.	Land Cover	Rn	G
1.	Pond	212	15
2.	Rice Fields Vegetation	208	17
3.	Fallow Rice Fields	195	20
4.	Industry	194	21
5.	Urban	194	20
6.	Rural	201	19
7.	Shrub	207	18
8.	Plantation	213	16

2. TOOLS AND METHODS

This research will be conducted with the selected research location, namely in the Denpasar City area, Bali, which is located at 8º40'37" LS and 115º12'36" E, as presented in Figure 1. Data collection and processing will be carried out from March to May 2023.

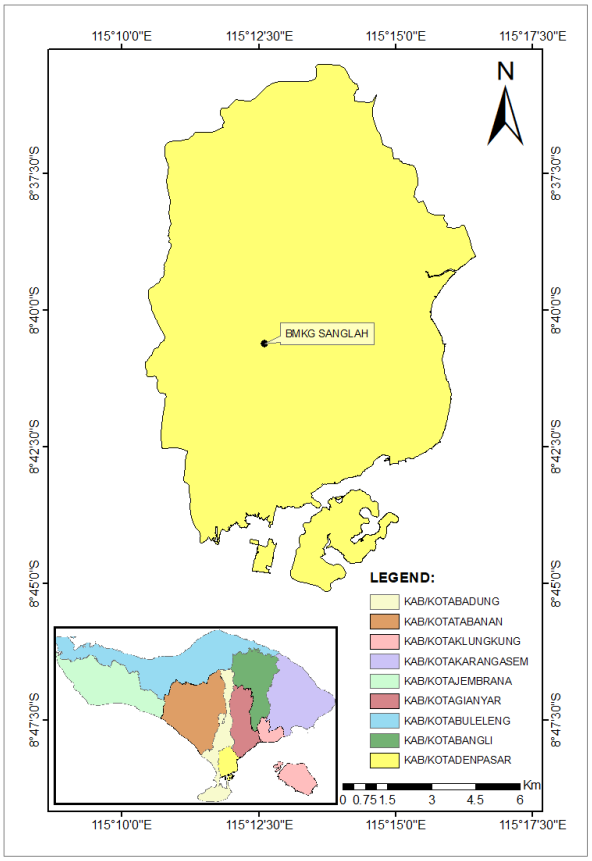

Figure 1 Map of the study area

2.1 Data Collection Methods

The data used in this study are satellite images of *the* Sentinel-3 SLSTR and Terra MODIS-LST thermal bands, as well as air temperature data from the Meteorology, Climatology and Geophysics Agency (BMKG) Sanglah Geophysical Station Denpasar in 2021. The collection of Sentinel-3 SLSTR satellite image data was carried out by downloading directly on the official website of the *Copernicus Open Hub* and taking Terra MODIS-LST satellite image data by

downloading on the official website of the *United States Geological Survey* (USGS). The tools used in this study are: Sentinel Application Platform (SNAP), ArcGIS 10.8, Microsoft Excel, and IBM SPSS Statistics.

2.2 Data Processing Methods

Data processing is carried out through several stages, namely, data collection, conversion of Sentinel-3 SLSTR and Terra MODIS-LST satellite images, cutting of research area images, and conversion of ESG on satellite images to air temperature (T_a).

2.3 Data Analysis Methods

The data analysis carried out includes correlation coefficients, t tests, and RMSE. In Natadiredja (2018) [14] the equation used to determine the value of the correlation coefficient (r) is like Equation (3):

$$r_{x_{sat}x_{ob}} = \frac{\sum_{i=1}^{n} (x_{sat\_i} - \bar{x}_{sat})(x_{ob\_i} - \bar{x}_{ob})}{\left(\sum_{i=1}^{n} (x_{sat\_i} - \bar{x}_{sat})^2 \sum_{i=1}^{n} (x_{ob\_i} - \bar{x}_{ob})^2\right)^{1/2}} \quad (3)$$

Information:

$r_{x_{sat}x_{ob}}$: Correlation coefficient between BMKG observation data and satellite data

x_{ob_i} : BMKG observation data in the i-th period with i = 1,2,3,..,n

$\bar{x}_{ob}$: Average value of BMKG observation data

x_{sat_i} : Results of satellite data in the i-th period with i = 1,2,3,..,n

$\bar{x}_{sat}$: Average value of satellite data results

n : Amount of data

According to Ahemaitihali and Zouji (2022) [15], the correlation coefficient (r) has values that range from -1 to +1.

2.3.1 t-test

In this study the t test was used to find out if there are differences between the measuring instruments used in this study, researchers used the error significance level (*alpha*) 5% (0.05). In performing the t-test, the hypotheses formulated for each independent variable are as follows:

1. Sentinel-3 satellite image with BMKG air temperature

H_0 : There is no significant difference between the air temperature measurement results of Sentinel-3 satellite images and BMKG air temperature.

H_1 : There is a significant difference between the air temperature measurement results of Sentinel-3 satellite images and BMKG air temperature.

2. Terra MODIS satellite image with BMKG air temperature

H_0: There is no significant difference between the air temperature measurement results of Terra MODIS satellite images and BMKG air temperature.

H_1 : There is a significant difference between the air temperature measurement results of Terra MODIS satellite images and BMKG air temperature.

Acceptance or rejection of this hypothesis test is carried out with the following criteria:

a. If the t value < t table then H_0 accepted and H_1 rejected (no significant difference).

b. If the t value > t table then H_1 accepted and H_0 rejected (significant difference).

2.3.2 Root Mean Square Error (RMSE) Calculation

Root Mean Square Error (RMSE) is a large error rate of prediction results, according to Obieogu et al (2020) [16] , Sandoval et al (2023) [17] , Moriasi et al (2007) [18], Guo et al (2017) [19] and Jierula et al (2021) [20] RMSE ranges from (0, +∞) and the smaller the RMSE value (close to zero), the higher the accuracy of the prediction model. In Natadiredja (2018) [14] the RMSE value can be calculated using the equation (4).

$$RMSE = \sqrt{\frac{\sum_{i=1}^{n} (x_{ob\_i} - x_{sat\_i})^2}{n}} \quad (4)$$

Information:

x_{ob_i} : BMKG observation data in the i-th period with i = 1,2,3,..,n

x_{sat_i} : Results of satellite data in the i-th period with i = 1,2,3,..,n

n : Amount of data

To determine the category of accuracy obtained from RMSE, RMSE value parameters are used. According to Oke et al (2020) [21] the RMSE value parameters can be seen in Table 4.

Table 4 RMSE value parameters

Parameters	Performance
RMSE < 0.009	Excellent prediction accuracy
0.009 < RMSE < 0.09	Good prediction accuracy
0.09 < RMSE < 0.5	Reasonable prediction
RMSE > 0.51	Inaccurate prediction

Source: Oke, et, al. 2020

2.4 Framework of Thought

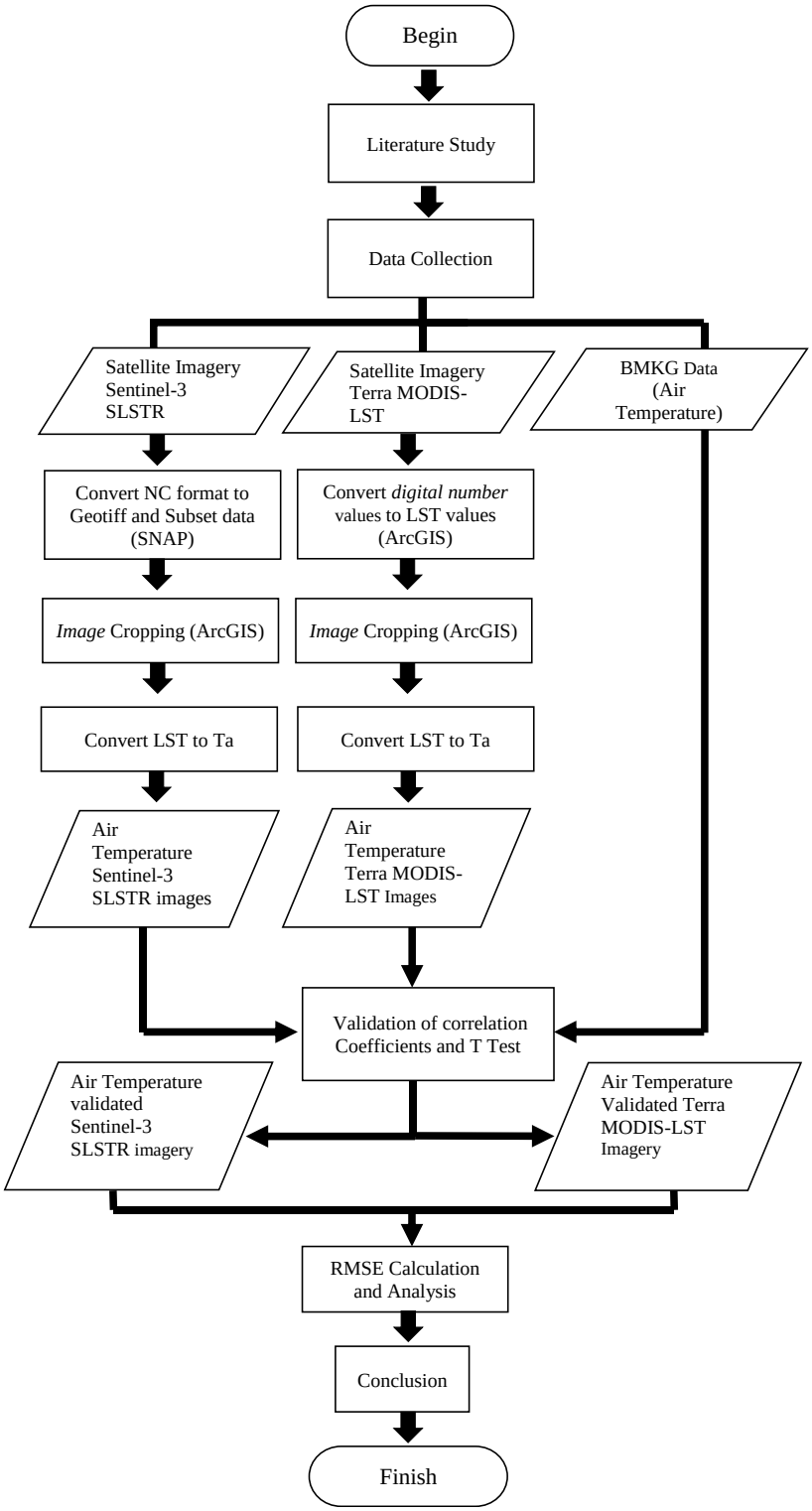

Figure 2. Frame of Mind

3. RESULTS AND DISCUSSION

3.1. Air Temperature Measurement Results of Sentinel-3 Satellite Image

Based on observations, it is known that in 32 observations of the 2021 period in the Denpasar area, the minimum temperature that can be detected by Sentinel-3 satellite images was 9.51°C on September 23, 2021 in the South Denpasar area, and the maximum temperature was 41.50°C on April 14, 2021 in the West Denpasar area. In addition to knowing the minimum and maximum temperatures, the air temperature at the point of the research location has also been obtained, then a graph can be formed, the Sentinel-3 air temperature pattern graph with BMKG air temperature (Figure 3) and the scatter plot graph (Figure 4). Figure 3 shows that the Sentinel-3 air temperature pattern graph almost follows the BMKG air temperature pattern chart, but it can be seen that there is an air temperature difference that causes the Sentinel-3 air temperature chart pattern to tend to be higher than the BMKG air temperature chart pattern. The largest difference in air temperature between the air temperature of the Sentinel-3 satellite image and the air temperature of BMKG was found on July 19, 2021, with a difference of 2.63. In Figure 4, it is known that the value of the coefficient of determination is 0.6038, so it can be known that Sentinel-3 satellite images can predict BMKG air temperature by 60.38%.

Through the results of the calculation of the correlation coefficient and t test, it can be seen that the air temperature of the Sentinel-3 satellite image with BMKG air temperature has a correlation coefficient value of 0.78, the value of the correlation coefficient is included in the very strong positive correlation category. In the results of the t test, it was found that in the air temperature of the Sentinel-3 satellite image with BMKG air temperature, the results of air temperature measurements were statistically insignificant. This is because the resulting t value is less than the t table ($-1.637 < 1.696$), so H_0 is accepted. This means that the air temperature

results of the Sentinel-3 satellite image and BMKG air temperature are not significantly different (statistically there is no significant difference). Insignificant t-test results can be due to the small number of samples, this statement is supported by Nurminen's (1997) research [22] which says that in large population groups, even small differences become statistically significant, whereas in small samples, clinically significant observations can remain statistically insignificant. The insignificant t-test results in this study are also supported by Xiong and Chen's (2017) research [23], with similar topics regarding temperature observations of Landsat satellite images and field observations that also produce statistically insignificant correlations.

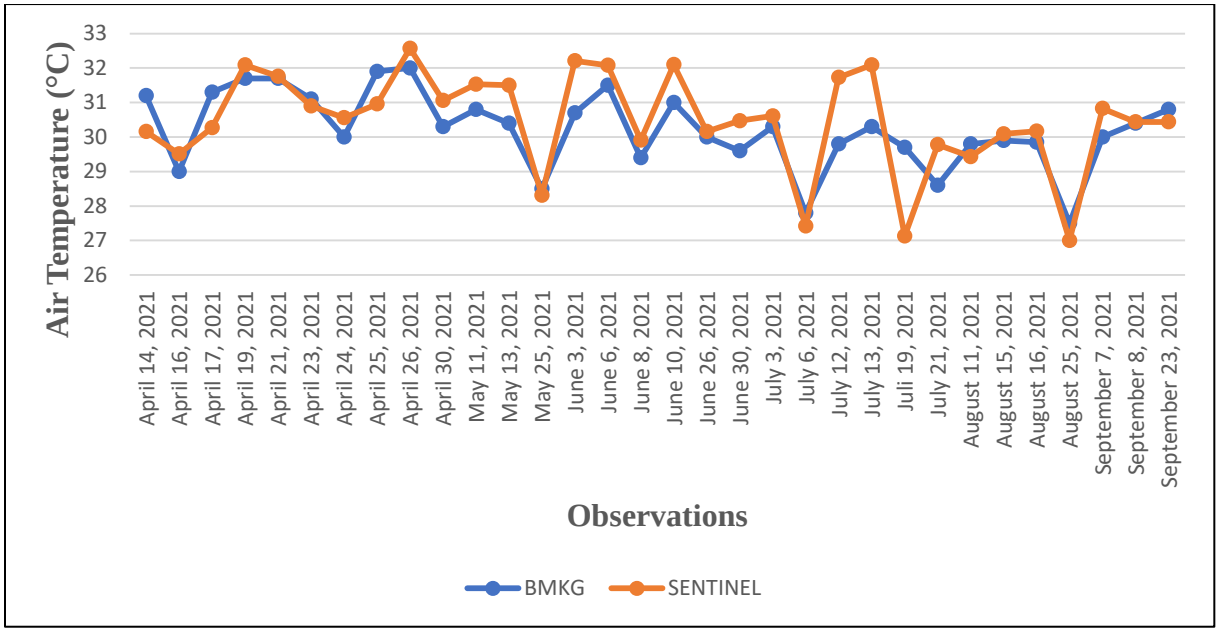

Figure 3 Sentinel-3 air temperature pattern with BMKG air temperature

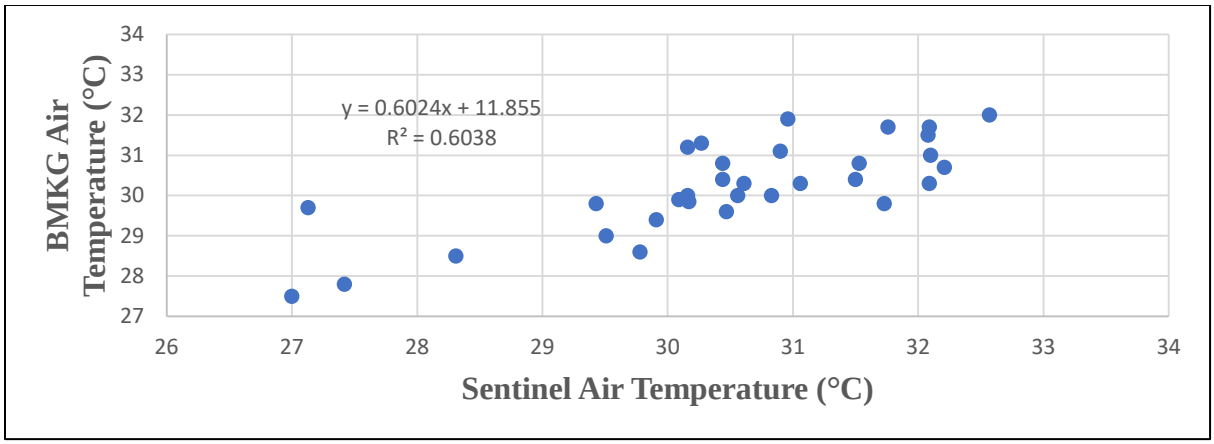

Figure 4 Scatter plot of Sentinel-3 air temperature with BMKG air temperature

3.2 Air Temperature Measurement Results Terra MODIS Satellite Image

From the processing results, it is known that in 32 observations of the 2021 period in the Denpasar area, the minimum temperature that can be detected by Terra MODIS satellite images was 20.57°C on September 23, 2021 in the South Denpasar area, and the maximum temperature was 37.08°C on April 16, 2021 in the West Denpasar area. In addition to knowing the minimum and maximum temperatures, the air temperature at the point of the research location has also been obtained. Figure 5 shows that the Terra MODIS air temperature pattern graph almost follows the BMKG air temperature pattern graph, the largest air temperature difference between the air temperature of Terra MODIS satellite images and BMKG air temperature is found on April 14, 2021, with a difference of 1.17. In Figure 6, it is known that the value of the coefficient of determination is 0.895, so it can be known that Terra MODIS satellite images can predict BMKG air temperature by 89.50%.

Through the results of the calculation of the correlation coefficient and t test, it can be seen that the air temperature of the Terra MODIS satellite image with BMKG air temperature has a correlation coefficient value of 0.95, the value of the correlation coefficient is included in the very strong positive correlation category. In the t-test results, it was found that the air

temperature of the Terra MODIS satellite image with the BMKG air temperature, statistically the air temperature results between the Terra MODIS satellite image and the BMKG air temperature were not significant. This is because the resulting t value is less than the t table (-5.824 < 1.696), so H_0 is accepted. This means that the air temperature of Terra MODIS satellite images and BMKG air temperature are not significantly different (statistically there is no significant difference). If there is a difference in minimum and maximum air temperatures obtained by each satellite image, it can be caused by atmospheric disturbances such as cloud cover or differences in spectral resolution owned by Sentinel-3 and Terra MODIS satellite images. This is supported by Cervest's (2020) article [24] and in Wang et al (2023) research [25] which says that the higher the spectral resolution, the better the ability of satellite image sensors to identify wavelengths. Terra MODIS has a very narrow bandwidth, so it can better distinguish subtle differences in surface reflections, and can better predict temperature.

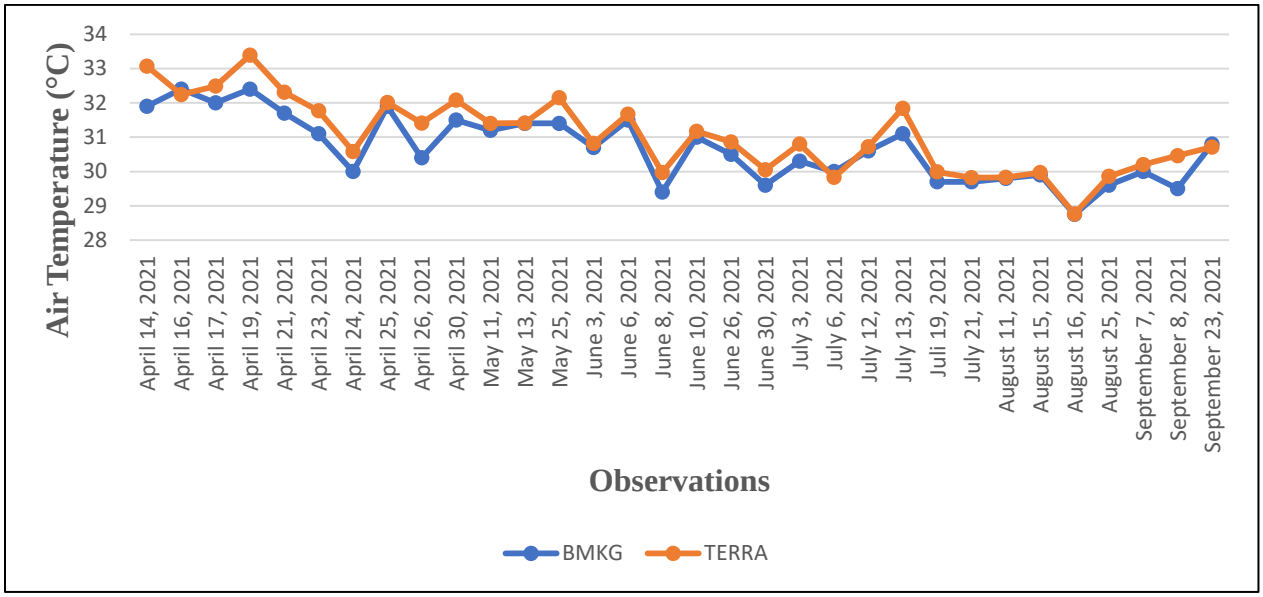

Figure 5 Terra MODIS air temperature pattern with BMKG air temperature

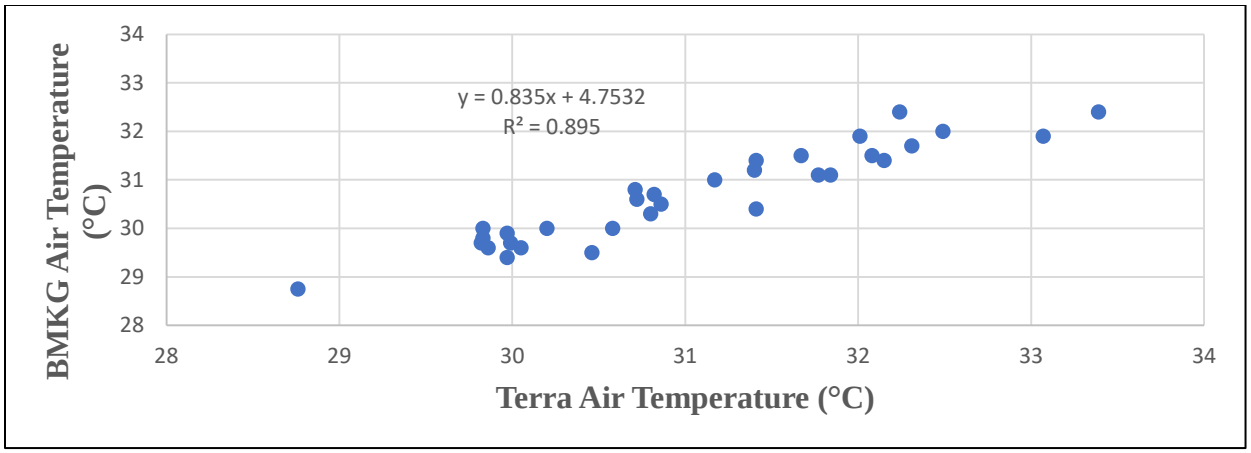

Figure 6 Scatter plot of Terra MODIS air temperature with BMKG air temperature

3.3 Results of Correlation Coefficient Calculation and Statistical Testing t

After the air temperature on the Sentinel-3 and Terra MODIS satellite images was successfully obtained, then validation and data analysis were carried out using correlation coefficient calculations and statistical tests t. The results of the calculation of the correlation coefficient and statistical testing t can be seen in Table 5.

Table 5 Results of correlation coefficient calculation and statistical testing t

No.	Variable	r Value	r Category	r^2 Value	t Value	t Table	Information
1.	Sentinel-3 with BMKG	0,78	Positive very strong	0,60	-1.637	1.696	No significant difference
2.	Terra MODIS with BMKG	0,95	Positive very strong	0,89	-5.824	1.696	No significant difference

3.4. RMSE Calculation Results

The RMSE calculation is performed using Equation 4. The results of the RMSE calculation can be seen in Table 6.

Table 6 RMSE Results

No.	Variable	RMSE value	Accuracy Rate Categories
1.	Sentinel-3 with BMKG	0,93	Good Accuracy Rate
2.	Terra MODIS with BMKG	0,51	Excellent Accuracy Rate

4. CONCLUSION

Based on the analysis that has been done, it can be concluded that:

1. The minimum temperature detected by Sentinel-3 satellite images from 32 observations was 9.51°C on September 23, 2021 and the maximum temperature was 41.50°C on April 14, 2021. Meanwhile, in Terra MODIS satellite images from 32 observations, the minimum temperature was 20.57°C on September 23, 2021 and the maximum temperature was 37.08 on April 16, 2021.

2. Terra MODIS satellite imagery has better accuracy to BMKG air temperature compared to Sentinel-3 satellite imagery. Terra MODIS imagery has a correlation coefficient value of 0.95 and an RMSE value of 0.51, while Sentinel-3 satellite imagery has a correlation coefficient value of 0.78 and an RMSE value of 0.93. So it can be noted that Terra MODIS satellite images are better used in air temperature observations than Sentinel-3 satellite images in the Denpasar area.

REFERENCE

[1]. Alfiandy, S., Imron, A.R., and Donaldi, S.P. 2022. Air Temperature Increase Pattern Based on BMKG and ERA5 Data in Central Sulawesi Province. *Journal of Forest Policy Analysis*. 19(1): 63-70

[2]. Hooker, J., Gregory, D., and Alessandro, C. 2018. A Global Dataset of Air Temperature Derived from Satellite Remote Sensing and Weather Stations. *Scientific Data*. 5(180246): 1-11

[3]. Faisol, A., Indarto., Elida, N., and Budiyono. 2018. Utilization of Satellite Imagery to Generate Air Temperature Information to Support Water Resources Management. *National Seminar in the framework of the 42nd Anniversary*.

[4]. Runke, W., Xiaoni, Y., Yaya, S., Chengyong, W., and Baokang, L. 2022. Study on Air Temperature Estimation and Its Influencing Factors in A Complex Mountainous Area. *PLOS ONE*. 17(8): 1-23

[5]. The European Space Agency. 2022. *Sentinel Online*. https://sentinels.copernicus.eu/web/sentinel/missions/sentinel-3. Retrieved January 19, 2023.

[6]. Mirnayani., Sry, K.R., Andi, N.A., and Atar, A.B. 2021. Utilization of Sentinel-3 Sea and Land Surface Temperature Radiometer (SLSTR) Morning and Night Image Data for Analysis of the Intensity of the Bahang Surface Island Phenomenon (Case Study: Bandung City). *Journal of Remote Sensing and Digital Image Data Processing*. 18(1): 15-25

[7]. Satrioajie, W.N. 2012. MODIS satellite imagery technology for sea surface temperature measurement. *Oceana*. 37(3): 1-9

[8]. Handayani, T, and Desyanti. 2019. Compression of Fashionable Terra Satellite Imagery using Shortwave Switching. *SATIN-Science and Information Technology*. 5(2): 1-8

[9]. Yang, J., Menenti, M., Krayenhoff, E.S., Wu, Z., Shi, Q., and Ouyang, X., 2019, Parameterization of Urban Sensible Heat Flux from Remotely Sensed Surface Temperature: Effects of Surface Structure, *Remote Sensing*, 11(1347).

[10]. Trebs, I., Mallick, K., Bhattarai, N., Sulis, M., Cleverly, J., Woodgate, W., Silberstein, R., Najera, N.H., Beringer, J., Meyer, W.S., Su, Z., and Boulet, G., 2021, The Role of Aerodynamic Resistance in Thermal Remote Sensing-Based Evapotranspiration Models, *Remote Sensing of Environment*, 264(112602).

[11]. Obisesan, O.E., and Jegede, O.O., 2020, Evaluation of Selected Parameterizations of Aerodynamic Resistance to Heat Transfer for the Estimation of Sensible Heat Flux at A Tropical Site in The Ile-Ife Nigeria, Ife Journal of Science, 24 (1): 95-108.

[12]. Desi. 2011. Application of Remote Sensing to Estimate Surface and Air Temperatures in Peatlands and Minerals Using Energy Balance Method (Study Area: Sampit, Central Kalimantan). Department of Geophysics and Meteorology. Bogor Agricultural University. *Thesis*

[13]. Wiweka. 2014. Surface and Air Temperature Patterns Using Multitemporal Landsat Satellite Imagery. *Ecolab Journal*. 8(1): 1-52

[14]. Natadiredja, S. 2018. Daily Rainfall Validation Based on Global Satellite Mapping of Precipitation (GSMAP) Data in Bali and Nusa Tenggara Regions. Faculty of Mathematics and Natural Sciences. Udayana University. *Thesis*

[15]. Ahemaitihali, A, and Zouji, D. 2022. Spatiotemporal Characteristics Analysis and Driving Forces Assessment of Flash Floods in Altay.*Water*. 4(331): 2-18

[16]. Obieogu, K.N., Aguele, F., and Chiemenem, L., 2020, Soft Computing Prediction of Oil Extraction from Huracrepitan Seeds, Kem. Ind, 69(11-12): 653-658.

[17]. Sandoval, A.D.O., Sorensen, J., Rodriguez, J.P., and Bharati, L., 2023, Hydrologic-hydraulic Assessment of SUDC Control Capacity Using Different Modelling Approaches A Case Study in Bogota Columbia, *Water Science and Technology*, 00(01): 1-21.

[18]. Moriasi, D.N., Arnold, J.G., Liew, M.W.V., Bingner, R.L., Harmel, R.D., Veith, T.L., Model Evaluation Guidelines for Systematic Quantification of Accuracy in Watershed Simulations, *American Society of Agricultural and Biological Engineers*, 50(3): 885-900.

[19]. Guo, P., Liu, T., Zhang, Q., Wang, L., Xiao, J., Zhang, Q., Luo, G., Li, Z., He, J., Zhang, Y., and Ma, W., 2017, Developing A Dengue Forecast Model Using Machine Learning A Case Study In China, *PloS Neglected Tropical Diseases*, 11(10).

[20]. Jierula, A., Wang, S., Oh, T.M., and Wang, P., 2021, Study on Accuracy Metrics for Evaluating the Predictions of Damage Locations in Deep Piles Using Artificial Neural Networks with Acoustic Emission Data, Applied Science, 11(2314).

[21]. Oke, E.O., Adeyi, B.I., Okolo, J.A., Adeyi, J., Ayanyemi, K.A., Osoh, T.S., Adegoke., 2020, Phenolic Compound Extraction from Nigerian Azadirachta Indica Leaves Response Surface and Neuro Fuzzy Modelling Performance Evaluation with Cuckoo Search Multi Objective Optimization, *Results in Engineering*, 8(100160).

[22]. Nurminen, M. 1997. Statistical Significance - A Misconstrued Notion in Medical Reseacrh. *Scand J Work Environ Health*. 23(2): 232-235

[23]. Xiong, Y., and Chen, F. 2017. Correlations Analysis between Temperatures from Landsat Thermal Infrared Retrievals and Synchronous Weather Observations in Shenzhen, China. *Remote Sensing Applications: Society and Environment*. 7: 40-48

[24]. Cervest. 2020. Remote Sensing of Planet Earth – Part 3: Fashionable vs Sentinel-2. https://cervest.earth/. Retrieved June 2, 2023

[25]. Wang, S., Feng, Y., Fu, D., Kong, L., Li, H., Han, B., and Lu, F. 2023. Stratospheric Temperature Observations by Narrow Bands Ultra-High Spectral Resolution Sounder from Nadir-Viewing Satellites. *Remote Sens*. 15(1967)